ISSN (Print) 1226-1750
ISSN (Online) 2233-6656
Journal of Magnetics 28(2), 172-180 (2023) https://doi.org/10.4283/JMAG.2023.28.2.172

Effect on the Sedimentation Stability of Magnetorheological Fluid by Micro-nano Composite System

Ji Jinjie[1], Wu Xiangfan[2]*, and Tian Zuzhi[1]

[1]*School of Mechatronic Engineering, China University of Mining and Technology, Xuzhou, P.R. China*
[2]*School of Mechanical and Electrical Engineering, Xuzhou University of Technology, Xuzhou, P.R. China*

(Received 17 November 2022, Received in final form 4 May 2023, Accepted 8 May 2023)

In magnetorheological devices, the magnetorheological fluids are inevitably in a zero-field state when the MR device is out of work. Long-term placement will lead to the sedimentation of MR fluids, reducing the performance of the magnetorheological device. A novel magnetorheological fluid was prepared by mixing microparticles and nanoparticles to solve this problem. After one-week placement, the sedimentation rate of the novel magnetorheological fluid is only 0.23 %, decreased by 88.5 % compared with general magnetorheological fluid. The novel magnetorheological fluid shows excellent sedimentation stability, keeping magnetorheological devices in good condition.

Keywords : magnetorheological fluid, sedimentation, micro-nano, composite system

1. Introduction

Magnetorheological (MR) fluid is a coarse dispersion system composed of soft magnetic particles, base carrier fluid, and additives [1]. Under an exciting magnetic field, MR fluid will transform from Newtonian fluid to a solid-like state, which is real-time, reversible, and controllable [2, 3]. MR fluid has been applied to damps [4-6], clutch [7, 8], brake [8], shock absorber [4, 5, 9], and servo valve [10, 11] because it has the advantages of quick response, low energy consumption, effortless control, good durability, wide operating temperature range, and long service life [12].

In MR devices, the MR fluids are inevitably in the zero-field state when the MR device is out of work, and long-term placement will lead to the sedimentation of MR fluids [13]. The sedimentation of MR fluids will degrade the performance of MR devices and even render MR devices a failure. With the broader application of MR fluids, the researcher has focused on improving the sedimentation stability of MR fluid and thus obtaining an MR fluid with sedimentation resistance.

The sedimentation is due to the density difference between carbonyl iron powders (CIPs) and base carrier fluid [2]. It is an excellent method to improve the sedimentation stability of MR fluid by coating CIPs with non-covalent and covalent. Miroslav [14] repaired the spherical CIPs covered with conductive polymer polypyrene in a ribbon-like shape, effectively improving MR fluid's sedimentation stability. Martin [15] designed two types of core-shell particles grafted with poly glycidyl methacrylate and prepared an MR fluid with the novel particles. The results show that the sedimentation stability of the MR fluid was considerably improved. Hu [16] coated the CIPs with poly butyl acrylate by surface-initiated atom transfer radical polymerization. On this basis, Hu prepared a novel MR fluid with controllable off-state viscosity and higher shear yield stress.

The sedimentation stability of MR fluid was also improved in previous work by adding particles of various shapes, 1D, and 2D. Martin [17] investigated the influence of carbon allotrope on sedimentation stability and dispersibility of MR fluids. It is found that carbon nanotubes can make MR fluid in sedimentation stability. Rachofsky [18, 19] prepared 2D magnetic Fe_3O_4/ZHS hybrid composite sheets, and core-shell ZnO/CI urchin-like dispersed particles based on the two-step microwave-assisted solvothermal synthesis. The MR effects were significantly improved when the novel particles were added to MR fluids. Abigail [20] found α-$Ni(OH)_2$ 2D

*Corresponding author: Tel: +86-13914876762
Fax: +86-0516-83590777, e-mail: wuxiangfan2022@163.com

sheets with aspect ratios of 25000 can increase saturation pressure by as much as 46 % when added as the anisotropic additive in MR fluids. Zhang [21] adopted plate-like graphene oxide particles as a gap filler for the carbonyl-iron-based MR fluid to improve its sedimentation stability.

Meanwhile, it is also a widely used method to improve the sedimentation stability of MR fluid by enhancing the properties of the soft magnetic particle itself or preparing a novel soft magnetic particle. Anupama [22] designed an unknown MR fluid by dispersing Ni-Zn ferrite sub-microspheres in silicone oil. The MR fluid was subjected to steady-state shear conditions at different magnetic fields. The results show that the values depend strongly on the physical properties of the particles, such as the particle size, size distribution (polydispersity), and saturation magnetization. Kim [23] prepared a novel carbonyl-iron-based MR fluid using rod-like CrO_2 nanoparticles as additives. Compared to the general CI-based MR fluid, the novel MR fluid exhibits remarkably higher yield behavior and excellent sedimentation stability. Syang-Peng [24] prepared CI-MWCNT by a mild ultrasonication method and prepared a CI-MWCNT-based MR fluid. The novel MR fluid has better MR effects and sedimentation stability than the general CI-based MR fluid. However, the high cost and complex preparation process limit its more comprehensive application. Tong [25] synthesized flower-like cobalt particles (FCP) and sphere cobalt particles (SCP), and the properties of the two kinds of MR fluids with the two types of particles were compared. The FCP-based MR fluid presents higher zero-field viscosity, field-induced yield stress, storage modulus, and sedimentation stability than the SCP-based samples. Shobhakar [26] prepared spherical NiO nanoparticles, by which the novel MR fluid was prepared. The experimental results show that the magnetic properties of synthesized composites are significantly improved, making MR fluids have excellent mechanical properties.

The above research has improved the sedimentation stability of MR fluid. However, the existing methods to improve the sedimentation stability of MR fluids are cumbersome and costly, which is not fit for broad applications. In this work, the anti-sedimentation way was further investigated for MR fluids. The micro-nano composite system was obtained for the soft magnetic particles of MR fluid by mixing microparticles and nanoparticles. A novel MR fluid with sedimentation resistance was prepared and tested on this basis. The novel MR fluid can be applied to more MR devices, which will keep MR devices always in good condition.

2. Materials and Methods

2.1. Test materials

2.1.1. Soft magnetic particles

The soft magnetic particle is applied to generate magnetic force under a magnetic field. Carbonyl iron powder (CIP) is the most commonly used soft magnetic particle to prepare MR fluid. It has high permeability and high-temperature stability, low coercivity, and excellent magnetization and demagnetization properties.

The CIPs applied to prepare MR fluid are usually microscale. However, the nanoscale particles can be mixed with microscale particles to form a micro-nano composite system with a lower density and particle size. Besides, the strong interaction between nanoparticles interferes with the aggregation of microparticles to create a more stable 3-dimensional structure, which can also help improve the

Table 1. Parameters of microparticle (CIPs).

Product Serial Number	Fe	C	O	N	D50	Loose density	Compacting density	Average particle size
MRF-R20	98.32%	0.015	1.35	0.315	2.362	1.49	3.17	1.55 μm

Table 2. Parameters of nanoparticle (Fe, Co, Ni, Fe_3O_4, Fe-Co-Ni).

Particle material	Average particle size (nm)	Purity	Specific surface area (m^2/g)	Loose density (g/cm^3)	Compacting density (g/cm^3)	Morphology	Color
Fe	<100	>99.9%	>7	0.48	7.845	Sphere	Black
Co	<100	>99.9%	>37	0.37	8.9	Sphere	Black
Ni	<100	>99.9%	>8	0.74	8.9	Sphere	Black
Fe_3O_4	<100	>99.9%	>7.26	0.77	5.1	Sphere	Black
Fe-Co-Ni	<100	>99.9%	>29.651	0.9	3.124	Sphere	Black

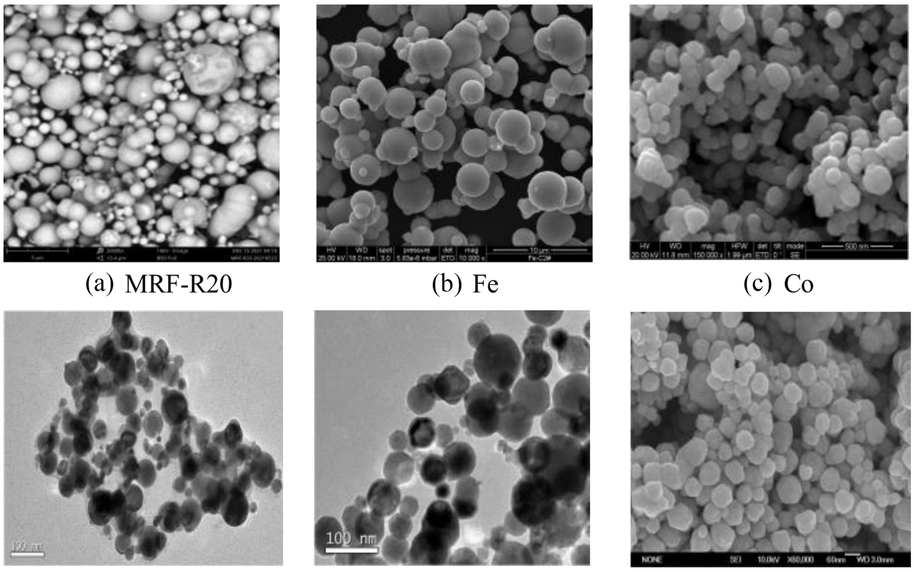

(a) MRF-R20 (b) Fe (c) Co

(d) Ni (e) Fe_3O_4 (f) Fe-Co-Ni

Fig. 1. Electron micrographs of magnetic particles: (a) MRF-R20, (b) Fe, (c) Co, (d) Ni, (e) Fe_3O_4, (f) Fe-Co-Ni.

sedimentation stability of MR fluids.

The microparticle in the micro-nano composite system is CIPs supplied by TIANYI (China), and their parameters are shown in Table 1. The nanoparticles (including Fe, Co, Ni, Fe_3O_4, Fe-Co-Ni) in the micro-nano composite system are supplied by QIYUE (China), and their parameters are shown in Table 2.

The scanning electron microscope (SEM) and transmission electron microscope (TEM) are applied to observe the surface morphology of the above materials, as shown in Fig. 1. As shown from Fig. 1, all six kinds of particles are in regular spheres. The radius of the above six types of particles is in a narrow range where the size of CIPs ranges from 1.5 to 2.5 μm, with an average particle size of approximately 1.55 μm. The average particle size of nanoparticles is less than 100 nm. The Van der Waals attraction between particles makes nanoparticles accumulate because the particles are small in size and have large specific surface areas.

2.1.2. Base carrier fluid

The base carrier fluid includes oil- and water-based carrier fluid [27]. Water has a lower viscosity, and thus the lower buoyancy cannot prevent particles from sedimentation. Besides, MR fluids, especially those in high-power MR devices, inevitably work at high temperatures because of the wall slip, energized coils and friction between particles. Water with poor thermal characteristics will evaporate at high temperatures, making MR fluids unstable. Therefore, oil-based is a better choice for preparing the MR fluids with sedimentation stability. The silicone oil is most commonly applied as the base carrier fluid for MR fluids, and the silicone oil was used to prepare the MR fluids with sedimentation resistance. Table 3 shows the parameters of silicone oil DOW CORNING (American) provided.

The thermostatic oil bath heated the silicone oil from 10 °C to 180 °C, of which the temperature interval is 10 °C. The silicone oil was kept at each temperature for 10 minutes to allow adequate heat exchange. Then the SNB-1T digital rotational viscometer by FANGRUI (China) was applied to measure the viscosity of silicone oil at different temperatures. The viscosity-temperature curve of the silicone oil is plotted in Fig. 2.

As can be seen from Fig. 2, the viscosity of silicone oil decreases with temperature rising. The viscosity decreases

Table 3. Parameters of silicone oil.

Name	Viscosity (cSt)	Purity	Flash point (°C)	Freezing point (°C)	Density (g/cm^3)	Surface tension	Appearance	Scent
PMX-200	100	99.5%	≥ 315	< -65	0.975	21	Colorless and transparent liquid	Odorless

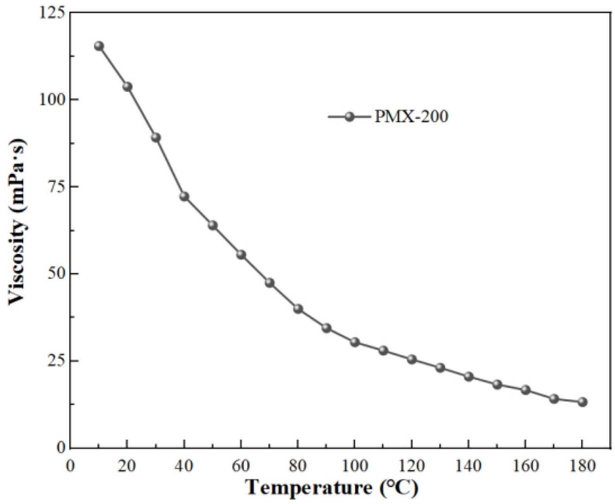

Fig. 2. The viscosity characteristics of PMX-200.

sharply in the temperature range from 10 °C to 60 °C, and then the decreasing trend slows down from 70 °C to 180 °C. The viscosity of silicone oil decreases by 88.5 % when the temperature rises from 10 °C to 180 °C. Besides, the viscosity index is 430, calculated from the viscosity-temperature curve. The higher viscosity index means the viscosity of silicone oil is less affected by temperature, which can keep MR fluid in good stability at high temperatures.

2.1.3. Surfactants

It was proved in the previous work [27] that the combination of the following surfactant can make MR fluid in excellent sedimentation stability:

1.5 wt% sodium lauryl phosphate

1.0 wt% compound fatty acid methyl ester sulfonate (compound MES)

1.5 wt% ethylene glycol monostearate

1.5 wt% glycerol monostearate

1 wt% hydrophobic fumed silica

Table 4 shows the information on the above surfactants.

2.2. Preparation method

The base-fluid-replacement method was applied to prepare the novel MR fluid with sedimentation resistance, and the preparation process is shown in Fig. 3.

The preparation process can be described as follows: (a) Mix soft magnetic particles with surfactants and anhydrous ethanol. (b) Stir and disperse the mixture with a stirrer and ultrasonic dispersion machine at 20 °C. (c) Dry the mixture in the vacuum drying oven at 60 °C, evaporating the anhydrous ethanol. (d) Grind and disperse the dried mixture for modified particles. (e) Mix the modified particles, thixotropic agent, and silicone oil for MR fluid.

2.3. Test methods

The significant density difference between base carrier fluid and soft magnetic particles leads to the sedimentation of MR fluid. In the absence of a magnetic field, the relative motion occurs between soft magnetic particles and base carrier fluid under the action of gravity. At this time, particles will settle from top to bottom in the container, and the sedimentation varies with time.

Kynch [28] described the sedimentation of MR fluids

Table 4. Information of surfactants.

Type	Name	Molecular formula	Company (Country)
Anionic surfactants	Sodium lauryl phosphate	$C_{12}H_{25}OPO_3Na_2$	ECOSOL (China)
	Compound MES	$RCH(SO_3M)COOCH_3$	ECOSOL (China)
Non-ionic surfactants	Ethylene glycol monostearate	$C_{20}H_{40}O_3$	ECOSOL (China)
	Glyceryl monostearate	$C_{21}H_{42}O_4$	ECOSOL (China)
Thixotropic agents	Hydrophobic fumed silica	SiO_2	DEGUSSA (Germany)

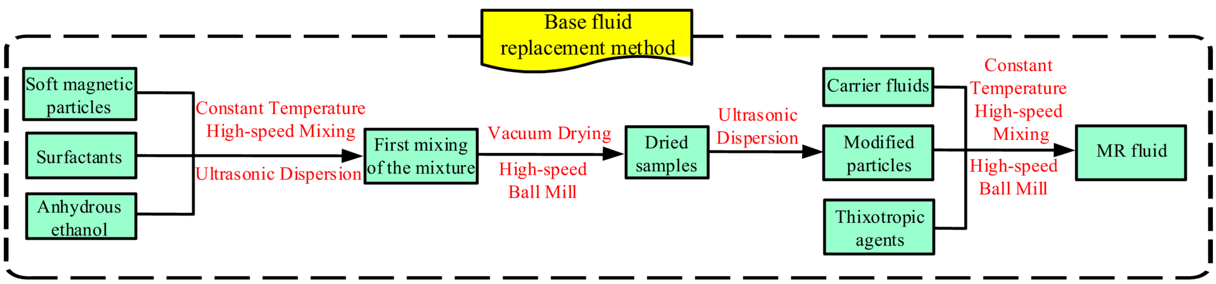

Fig. 3. (Color online) Preparation process of MR fluid.

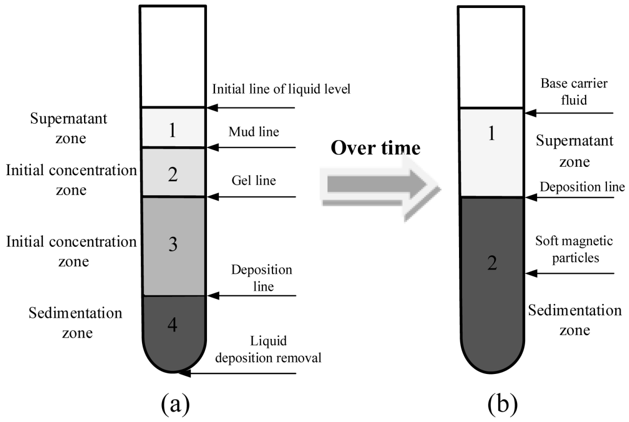

Fig. 4. Sedimentation scheme of MR fluid: (a) initial settlement, (b) full sedimentation.

by layered sedimentation theory, as shown in Fig. 4. The MR fluid after placement can be divided into a supernatant zone, initial concentration zone, variable concentration zone, and deposition zone, which is distinguished by mud line, gel line, and deposition line, as shown in Fig. 4(a). After the complete sedimentation, the MR fluid only contains the supernatant and deposition zones, as shown in Fig. 4(b).

The gravitational sedimentation theory can explain the sedimentation of MR fluid. The following assumptions are made to simplify the analysis: (a) All particles are made of the same material and are spheres of the same size. (b) The Brownian force can be ignored.

The soft magnetic particles are uniformly dispersed in the base carrier fluid without a magnetic field. At this time, the particles are subjected to gravity, buoyancy, and fluid resistance, as shown by equations (1), (2), and (3).

$$G = \frac{4}{3}\pi\left(\frac{d}{2}\right)^2 g\rho = \frac{\pi}{6}\rho g d^3 \tag{1}$$

$$F_f = \frac{4}{3}\pi\left(\frac{d}{2}\right)^2 g\rho_0 = \frac{\pi}{6}\rho_0 g d^3 \tag{2}$$

$$f = A\varepsilon\frac{\rho_0 u^2}{2} \tag{3}$$

where G is the gravity on soft magnetic particles. d is the average size of soft magnetic particles. ρ is the density of soft magnetic particles. g is gravitational acceleration. F_f is the buoyancy of soft magnetic particles in carrier fluid. ρ_0 is the density of base carrier fluid. f is the fluid resistance of soft magnetic particles. ε is the fluid damping coefficient. A is the surface area of soft magnetic particles. u is the sedimentation velocity of soft magnetic particles.

The soft magnetic particles move downward at a uniform speed when sedimentation occurs. At this time, the particles are subjected to a balanced force, as shown by equation (4).

$$G = F_f + f \tag{4}$$

In combination with equations (1), (2), (3), and (4), the sedimentation velocity of soft magnetic particles u can be obtained, as shown by equation (5).

$$u = 2\sqrt{\frac{gd(\rho-\rho_0)}{3\varepsilon\rho_0}} \tag{5}$$

Besides, the sedimentation velocity of the soft magnetic particles in the MR fluid can also be calculated by the Stokes formula, as shown by equation (6).

$$v = \frac{2d^2 g(\rho-\rho_0)}{9\eta} \tag{6}$$

where η is the viscosity of base carrier fluid.

The following conclusions can be obtained by comparing equations (5) and (6):

a) The sedimentation velocity of soft magnetic particles is proportional to the density difference between soft magnetic particles and a base carrier fluid.

b) The sedimentation velocity is proportional to the average particle size.

c) The sedimentation velocity is inversely proportional to the density and viscosity of the base carrier fluid.

Based on the above conclusions, the sedimentation of MR fluid can be restrained by reducing the density difference between soft magnetic particles and a base carrier fluid. However, the increase in viscosity or density of base carrier fluid will worsen the fluidity of MR fluid, so it is an excellent method to improve the sedimentation of MR fluid by reducing the density and size of soft magnetic particles.

3. Results and Discussion

3.1. Optimum particle material combination

Based on the preparation method, several MR fluid samples were prepared to find the optimum soft magnetic particle combination for the novel MR fluid with sedimentation resistance. In the prepared MR samples, the base carrier fluid and surfactant were described in Chapter 2, while the particle information of each sample is shown in Table 5. The mass fraction of soft magnetic particles is 50 wt%.

Table 5. Different material combinations in micro-nano composite systems.

Number	Material combinations
A	CIPs
B	CIPs and Fe_3O_4
C	CIPs and Fe
D	CIPs and Co
E	CIPs and Ni
F	CIPs and Fe-Co-Ni

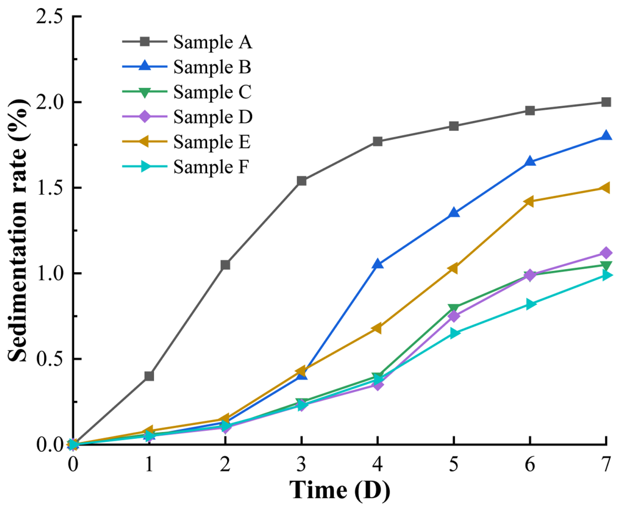

Fig. 5. (Color online) Sedimentation rates of MR fluid samples with different material combinations.

3.1.1. Sedimentation stability

The prepared MR fluid samples were placed for one week, and the placement-observation method was applied to calculate the sedimentation rates of MR samples. Fig. 5 shows the sedimentation rates of MR fluids with different material combinations.

It can be seen from Fig. 5 that the MR fluids with the micro-nano composite system have better sedimentation stability than the available MR fluid with CIPs. After one-week placement, the sedimentation rate is 2 % for general MR fluid (sample A). At the same time, it is only 0.99 % for sample F. Compared with sample A, the sedimentation stability of sample F significantly improves by 50.5 %. As all the soft magnetic particle combinations can bring better sedimentation for MR fluid, they can be applied to test other properties required by MR fluids.

3.1.2. Magnetization characteristic

The magnetic property is the most critical parameter for soft magnetic particles because soft magnetic particles are applied to generate magnetic force under a magnetic field. The different materials with magnetic properties significantly influence the mechanical properties of MR fluids. The MPMS 3 by QUANTUM DESIGN (America) was applied to measure the magnetic properties of the particle combinations in Table 5. Fig. 6 shows the hysteresis curves of particle groups.

As shown in Fig. 6, the six material groups have excellent magnetization performance where there is no noticeable hysteresis. Thus, the six materials groups can all be applied to prepare an MR fluid. The magnetization strength of the composite system increases with magnetic field strength, but the increasing trend slows down. Under the magnetic field from 0 to 280 kA/m, the magnetization strength increases approximately linearly with magnetic field strength, while it gradually increases in the magnetic field strength from 280 kA/m to 400 kA/m. The magnetization strength trend to a fixed value when the magnetic

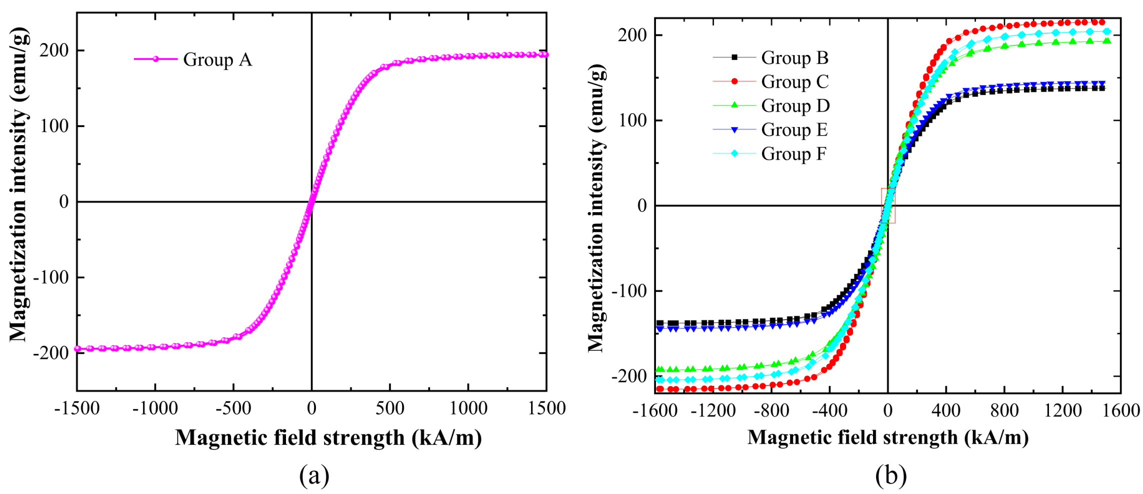

Fig. 6. (Color online) Hysteresis curves of particle groups: (a) group A, (b) group B, C, D, E and F.

field strength reaches 500 kA/m.

The particle with high saturation magnetization strength has a high permeability, which can make MR fluid with high shear yield stress and quick response under the same magnetic field.

It is shown that the order of the magnetization strength under the same magnetic field is group C > group F > group A > group D > group E > group B. As stated above, the particles with higher saturation magnetization strength can make MR fluid with a higher shear yield stress, shorter response time, and lower hysteresis loss. Therefore, the novel MR fluid by CIPs and Fe-Co-Ni will have a better magnetic performance than the general MR fluid by pure CIPs.

3.2. Optimum particle content ratio

3.2.1. Sedimentation rate

Based on the preparation method, several MR fluid samples were prepared to find the optimum particle content ratio for the novel MR fluid with sedimentation resistance. In the prepared MR samples, the base carrier fluid and surfactant were described in Chapter 3, while the particle information of each sample is shown in Table 6. The mass fraction of soft magnetic particles is 50 wt%.

The prepared MR fluid samples were placed for one week, and the placement-observation method was applied to calculate the sedimentation rates of MR samples. Fig. 7 shows the sedimentation rates of MR fluid samples with different material combinations.

It can be seen from Fig. 7 that the MR fluids with more nanoparticles have lower sedimentation rates, exhibiting better sedimentation stability. When the nanoparticles account for 70 % of soft magnetic particles (sample 5), the sedimentation rate of the sample is only 0.23 % after one-week placement. The sedimentation rate of the novel MR fluid decreased by 88.5 % compared with that of the general MR fluid shown in Fig. 7, showing excellent sedimentation stability. Based on the above research, the 50 wt% and 70 wt% fractions of particles (30 % CIPs and 70 % Fe-Co-Ni) are used to prepare MR fluid, respectively. The prepared MR fluid samples were placed for one week, and the placement-observation method was applied to calculate the sedimentation rates of the two MR samples. After one-week placement, there is no sedimentation in the MR fluid sample with a mass fraction of 70 wt%. However, the MR sample cannot flow or be injected into MR devices.

3.2.2. The rheological behavior

The SNB-1T digital rotational viscometer was applied to measure the zero-field viscosity of the samples

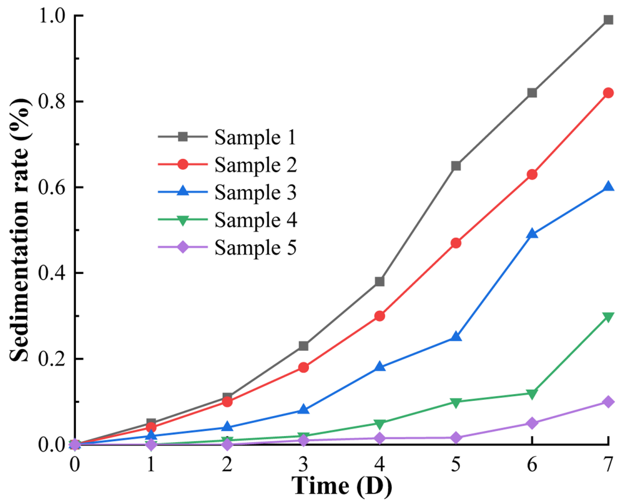

Fig. 7. (Color online) Sedimentation rates of MR fluid samples with different particle content ratio.

Table 6. Different mass fraction of nanoparticles in micro-nano composite system.

Sample number	Sample composition	
	Microparticles	Nanoparticles
1	CIPs (90 %)	Fe-Co-Ni (10 %)
2	CIPs (80 %)	Fe-Co-Ni (20 %)
3	CIPs (70 %)	Fe-Co-Ni (30 %)
4	CIPs (50 %)	Fe-Co-Ni (50 %)
5	CIPs (30 %)	Fe-Co-Ni (70 %)

prepared based on the compositions in Table 6.

Fig. 8(a) shows the zero-field viscosity of the MR fluid samples at room temperature (20 °C). As seen in Fig. 8, the viscosity of MR fluid samples by the micro-nano composite system is higher than that by CIPs at room temperature. Besides, the zero-field viscosity of MR samples increases with the content of nanoparticles when the mass fraction of particles is the same. Fig. 8(a) shows that the zero-field viscosity of MR samples is inversely proportional to the sedimentation rate. In the five samples by the micro-nano composite system, sample 4 and sample 5 have an even higher zero-field viscosity, which is 3 and 8 times higher than the general MR fluid by CIPs. When the viscosity is much higher, the MR fluid is in poor fluidity, and thus it cannot be injected into MR devices. Therefore, samples 2, 3, and 4 with suitable zero-field viscosity can be applied to test other performances.

The rotational rheometer MCR 302 equipped with MRD 170 by ANTON PAAR (Austria) was used to obtain the rheological curves of samples 1, 2, and 3 and the available MR fluid (sample A). The Herschel-Bulkley

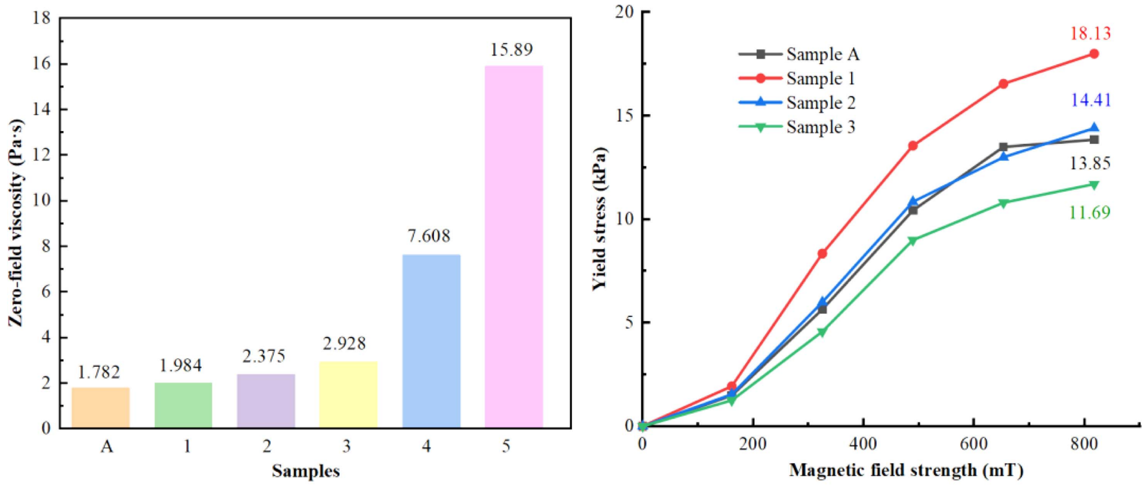

(a) Zero-field viscosity of MR fluid samples **(b) Shear yield stress of MR fluid samples**

Fig. 8. (Color online) The rheological behavior of MR fluid samples.

[29] model with better fitting effects was applied to obtain the shear yield stress of each MR sample, as shown in Fig. 8(b).

It can be seen from Fig. 8(b) that the shear yield stress of all MR samples increases with magnetic field strength. In the same magnetic field, MR fluids with a few nanoparticles have higher shear yield stress because nanoparticles fill the space between microscale CIPs, forming more vital particle chains for anti-shear. However, the shear yield stress decrease when the MR fluid contains more nanoparticles. At this time, the average radius of soft magnetic particles decreases sharply, and thus particles are subject to lower magnetic force in the same magnetic field. In the magnetic field of 817 mT, the shear yield stress of sample 1 is 18.13 kPa, increasing by 31% compared with general MR fluid (sample A), which has better mechanical properties.

4. Conclusions

The sedimentation of MR fluid can be restrained by reducing the density difference between soft magnetic particles and a base carrier fluid. The micro-nano composite system was obtained for the soft magnetic particles of MR fluid with sedimentation resistance by mixing microparticles and nanoparticles.

The material formula of MR fluid with sedimentation resistance is as follows: (a) The soft magnetic particles are 30 % microscale CIPs and 70 % nanoscale Fe-Co-Ni particles, and their mass fraction is 50 wt%. (b) The base carrier fluid is dimethyl silicone oil. (c) The surfactant combination is 1.5 wt% sodium lauryl phosphate, 1.0 wt% compound MES, 1.5 wt% ethylene glycol monostearate, 1.5 wt% glycerol monostearate, and 1 wt% hydrophobic fumed silica.

After one-week placement, the sedimentation rate of the novel MR fluid was only 0.23 %, decreased by 88.5 % compared with general MR fluid. The novel MR fluid shows excellent sedimentation stability, which can be applied to more MR devices. The viscosity of MR fluid samples by the micro-nano composite system is higher than that by CIPs at room temperature. The zero-field viscosity of MR samples increases with the content of nanoparticles when the mass fraction of particles is the same. The rotational rheometer MCR 302 equipped with MRD 170 by ANTON PAAR (Austria) and the Herschel-Bulkley [29] model with better fitting effects was applied to obtain the shear yield stress of each MR sample. The shear yield stress of all MR samples increases with magnetic field strength. In the same magnetic field, MR fluids with a few nanoparticles have higher shear yield stress because nanoparticles fill the space between microscale CIPs, forming stronger particle chains for anti-shear. In the magnetic field of 817 mT, the shear yield stress of the sample is 18.13 kPa, increasing by 31 % compared with general MR fluid (sample A), which has better mechanical properties.

Acknowledgements

This research was supported by the National Natural Science Foundation of China (51875560, 52005426), Jiangsu Natural Science Foundation (BK20190155), and the Priority Academic Program Development of Jiangsu Higher Education Institutions.

References

[1] Z. Z. Tian, X. F. Wu, X. M. Xiao, and F. Chen, J. Magn. **24**, 634 (2019).
[2] M. Xu, K. L. Zhang, Y. L. Yang, T. X. Cheng, and G. D. Zhou, Phys. Status Solidi A **219**, 2100759 (2022).
[3] F. Chen, Z. Z. Tian, X. F. Wu, S. Y. Wang, and H. Li, J. Magn. **23**, 99 (2018).
[4] T. Kumar, R. Kumar, and S. C. Jain, Lect. N Mech. Eng. 1645 (2022).
[5] J. Hou, J. C. Niu, Y. J. Shen, S. P. Yang, and W. J. Zhang, J. Vib. Control. 10775463211023368 (2021).
[6] S. Acharya, T. R. Saini, and H. Kumar, J. Braz. Soc. Mech. Sci. **41**, 392 (2019).
[7] X. F. Wu, C. H. Huang, Z. Z. Tian, and J. J. Ji, Smart Mater. Struct. **28**, 055021 (2019).
[8] M. A. Fernandez and J. Y. Chang, Smart Mater. Struct. **30**, 065024 (2021).
[9] R. Aboutalebi, M. Eshaghi, and A. Taghvaeipour, J. Intel. Mat. Syst. Str. **32**, 781 (2021).
[10] X. C. Yin, C. Wu, S. Wen, and J. T. Zhang, Ieee T Instrum. Meas. **70**, 7504111 (2021).
[11] M. Bialek, C. Jedryczka, and A. Milecki, Energies **14**, 6541 (2021).
[12] H. P. Li, I. Jonkkari, E. Sarlin, and F. Chen, Rheol. Acta. **60**, 719 (2021).
[13] A. V. Anupama, V. B. Khopkar, V. Kumaran, and B. Sahoo, Phys. Chem. Chem. Phys. **20**, 20247 (2018).
[14] M. Mrlik, M. Sedlacik, V. Pavlinek, P. Bazant, P. Saha, P. Peer, and P. Filip, J. Appl. Polym. Sci. **128**, 2977 (2013).
[15] M. Cvek, M. Mrlik, M. Ilcikova, T. Plachy, M. Sedlacik, J. Mosnacek, and V. Pavlinek, J. Mater. Chem. C **3**, 4646 (2015).
[16] B. Hu, A. Fuchs, S. Huseyin, F. Gordaninejad, and C. Evrensel, Polymer **47**, 7653 (2006).
[17] M. Cvek, M. Mrlik, R. Moucka, and M. Sedlacik, Colloid Surface A **543**, 83 (2018).
[18] M. Machovsky, M. Mrlik, T. Plachy, I. Kuritka, V. Pavlinek, Z. Kozakova, and T. Kitano, Rsc. Adv. **5**, 19213 (2015).
[19] M. Machovsky, M. Mrlik, I. Kuritka, V. Pavlinek, and V. Babayan, Rsc. Adv. **4**, 996 (2014).
[20] A. Rendos, R. Li, S. Woodman, X. Ling, and K. A. Brown, Chemphyschem. **22**, 431 (2021).
[21] W. L. Zhang, S. D. Kim, and H. J. Choi, IEEE T Magn. **50**, 2500804 (2014).
[22] A. V. Anupama, V. Kumaran, and B. Sahoo, Powder Technol. **338**, 190 (2018).
[23] M. H. Kim, K. Choi, J. D. Nam, and H. J. Cho, Smart Mater. Struct. **26**, 095006 (2017).
[24] S. P. Rwei, J. W. Shiu, R. Sasikumar, and H. C. Hsueh, J Solid State Chem. **274**, 308 (2019).
[25] Y. Tong, X. F. Dong, and M. Qi, Smart Mater. Struct. **26**, 025023 (2017).
[26] B. H. Shambharkar and S. S. Umare, J. Appl. Polym. Sci. **122**, 1905 (2011).
[27] F. Chen, H. P. Li, M. M. Han, Z. Z. Tian, and A. M. Li, Mater. Manuf. Process **35**, 1077 (2020).
[28] G. J. Kynch, Trans Faraday Soc. **48**, 166 (1952).
[29] H. P. Li, I. Jonkkari, E. Sarlin, and F. Chen, Braz. J. Phys. **51**, 1735 (2021).